ARTICLE

Formation of Close-Packed Nanoparticle Chains

Leonid V. Govor*

Institute of Physics, University of Oldenburg, D-26111 Oldenburg, Germany

ABSTRACT The self-assembly of $CoPt_3$ particles (diameter 6 nm) into low-dimensional ordered arrays results from phase separation in a hexane solution containing nanoparticles, hexadecylamine, and water. The evaporation of hexane from the thin film of solution initiates the formation of a water layer on the solid substrate. Subsequent dewetting of this water layer leads to the formation of water droplets. The nanoparticles follow the motion of the contact line of the dewetting water layer and thus assemble into ordered arrays at the periphery of the water droplets.

KEYWORDS: self-assembling • nanoparticle chain • phase separation • dewetting

1. INTRODUCTION

Nanoparticles have been the subject of intensive study because of their unique electronic properties. One of the keys to using the nanoparticles in future electronic technology is their controllable and precise assembly into ordered low-dimensional structures. Compared to randomly distributed particle arrays, ordered particle structures are better candidates for most practical applications. During the past few years, the electronic properties of individual particles (1) as well as those of two- and three-dimensional arrays have been studied extensively (2−4). Recently, the charge transport through quasi-one-dimensional arrays of nanoparticles (containing four chains of particles; particle diameter 5.5 nm) was investigated experimentally (5). So far, no experimental studies are available on truly one-dimensional (1D) arrays of particles (containing only one or two chains). The practical manufacture of such arrays makes it possible to study, for example, the electronic hopping transport in 1D array of nanoparticles (6−8).

The aggregation of nanoparticles into ordered 1D structures was undertaken in several papers. Wyrwa et al. (9) described the 1D arrangements of metal nanoparticles formed by self-assembly processes at the phase boundary between water and dichloromethane. Huang et al. (10) showed that the 1D chains of single-particle thickness can be readily deposited on a substrate from a dilute Langmuir−Blodgett particle monolayer via a stick−slip motion of the water−substrate contact line. Suematsu et al. (11) observed that nanoparticles self-assembled into the ring-shaped structures containing two, three, or more particle chains, prepared by casting a toluene solution composed of polystyrene and silver nanoparticles. Khanal and Zubarev (12) found out that gold nanorods dispersed in dichloromethane can be organized into 1D circular arrays around the circumferences of water droplets located on the surface of the solution film.

The simple procedure presented here for aggregation of nanoparticles into ordered arrays is one of some advantages provided by instability phenomena developing in an evaporating bilayer formed via phase separation in a thin film of mixed polymer solutions containing nanoparticles (13, 14). There, solvent evaporation from two layers first led to decomposition of the top solution layer [hexane−hexadecylamine (HDA)-rich layer] into micrometer-sized droplets, while the bottom layer (amyl acetate−nitrocellulose (NC)-rich layer) did not become unstable and dried as a continuous film. As a result, the nanoparticles were assembled partly into a ring along the edges of HDA droplets and partly were distributed irregularly inside the droplets. In other words, the ordering of nanoparticles into ringlike structures was performed via the instability of the top layer. When the evaporation of the solvent from the supporting bottom layer is inhomogeneous, the solid aggregates located on its surface can be connected into ordered structures, for example, into treelike patterns (15), while the bottom layer dries as a continuous film.

In the present work, the instability phenomenon developed in the bottom layer (of the bilayer) was used for the ordering of nanoparticles. It was found that the self-assembly of nanoparticles into ordered arrays containing one, two, or three particle chains results from phase separation in the thin film of the hexane solution containing particles, HDA, and water. During hexane evaporation from the solution film on the solid substrate, the film transforms into a bilayer composed of a hexane layer on the water layer. The hexane layer dewets the surface of the water layer as a continuous film. During dewetting and evaporation of the hexane layer, most nanoparticles and HDA existing in the hexane layer adsorb on the surface of the water layer (nanoparticles and HDA are not soluble in water). The water layer covered by nanoparticles and HDA dewets the surface of the NC-coated substrate and decomposes into droplets. During dewetting, the particles locate at the contact line of the dewetted water layer (i.e., the interface between air, water, and NC layers)

* E-mail: leonid.govor@uni-oldenburg.de.
Received for review October 29, 2008 and accepted January 16, 2009
DOI: 10.1021/am800151e

Published on Web 02/05/2009

and follow its motion. Finally, during the formation of water droplets, the particles order along their edges.

It should be noted that no binary solution for the formation of a bilayer was used in the present work. The small volume of water in solution is an admixture in hexane but not a solvent for nanoparticles and HDA. As a result, the nanoparticles can only order into ringlike structures along the edges of the water droplets, but they cannot be located inside the latter compared to results obtained in refs 13 and 14.

2. EXPERIMENT

Hexane solutions with concentrations of 2.4×10^{12} and 3.1×10^{12} cm^{-3} of $CoPt_3$ particles (diameter 6 nm, stabilized with HDA (16)) were used in the present experiments. Moreover, each solution of particles contains additional HDA and water with concentrations of 1.0×10^{-3} and 1.0×10^{-2} vol %, respectively. According to the specification provided by the producer (AppliChem GmbH), hexane itself contains a maximum of 5×10^{-3} vol % of water; i.e., the total concentration of water in the solutions amounts to a maximum of 1.5×10^{-2} vol %. In general, the solubility of water in hexane at 20 °C is 2.8×10^{-2} vol % (4.27×10^{-2} mol %) (17), and therefore it was assumed that additional water was dissolved completely in the hexane solution of nanoparticles. The additional water in the solution plays the role of ordering nanoparticles into rings via the formation of water droplets after hexane evaporation, where the additional HDA covers the surfaces of the water droplets. This enables the position of the particle rings to be observed by an optical light microscope after water evaporation and, consequently, the particle chains to be placed between two electrodes for electronic transport analysis. In other words, the additional HDA plays the role of markers for the nanoparticle rings.

Thin films were prepared at ambient conditions by spreading the solution on (a) a silicon substrate covered with a NC film (thickness 100 nm) and (b) transmission electron microscopy (TEM) grids covered with a NC film (thickness 100 nm). It was found that the patterns formed on both substrates were similar. Because the volume of the initially deposited drop was 3 μL, the total thickness of the resulting solution layer with diameter 7 mm spread-out on the substrate can be estimated to be about 78 μm. The diameter of the spread solution layer remained constant for a time span of about 17 s and then decreased quickly to the center of the spreading area. The total time span between the casting of the solution and full drying of hexane amounted to about 20 s. The temporal development of the drying process of the solution layer was observed by light microscopy (magnification 500×). After evaporation of hexane and drying, the topography of the films was analyzed by atomic force microscopy (AFM; Dimension 3100, Digital Instruments). The AFM tapping mode and the "Nanosensors" SSS-NCHR AFM tips (typical radius of curvature of 2 nm; spring constant of 42 N/m) were used. The arrangement of the $CoPt_3$ particles was studied by TEM (Zeiss EM 902).

3. EXPERIMENTAL RESULTS

Figure 1a presents the typical dewetting process and clearly demonstrates that the dewetting system consists of two layers: the top hexane layer (*h*) dewets on the surface of the lower water layer (*w*), and that dewets on the surface of the NC/silicon substrate (*s*). During the dewetting process, the hexane layer remains the smooth film, while the water layer deforms at the beginning into the cellular structure, which then decomposes into droplets. Here, it is of interest

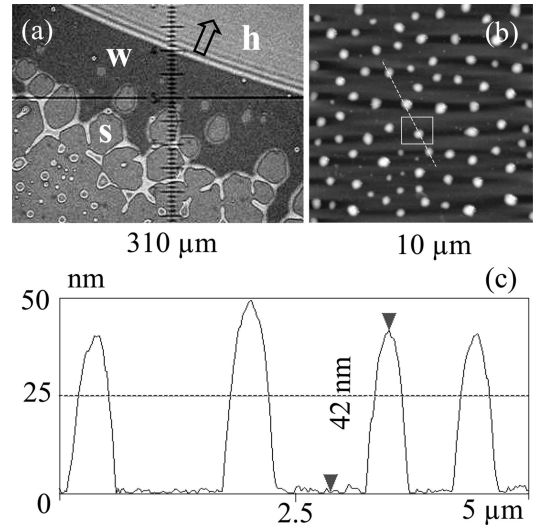

FIGURE 1. (a) Typical optical micrographs for retraction of the phase-separated layers of hexane (denoted as *h*) and water (denoted as *w*) on the NC/silicon substrate (denoted as *s*). An arrow illustrates the dewetting direction of the hexane layer. (b) AFM height image of water droplets located on a NC film. (c) Profile analysis of the scan taken along the dashed line indicated in part b.

to note a few special features observed in the described experiment. The dewetting of the thin water layer always started at the periphery of the spread film area and proceeded radially toward its center, building the droplet pattern. In this experiment, solutions containing either 0.015 or 0.005 vol % of water were used. The phase separation in the cast solution films appears in both cases, and the structure of the water droplets does not significantly depend on the presence or absence of HDA in the solution (for HDA concentrations up to 0.001 vol %). The time span necessary for dewetting and the total evaporation of the hexane layer amounted to about 3 s, whereas the water droplets could be observed during a few minutes (without HDA in solution). This time increases to a few days if the solution contains HDA. That means that, during dewetting and evaporation of hexane, HDA existing in hexane adsorbs on the water surface. As a consequence, the evaporation of water from water droplets covered by HDA is suppressed, and these droplets can be observed for a long time after decomposition of the water layer has taken place. It was found that similar droplet structures were formed in a closed desiccator in the presence of a hygroscopic P_2O_5 powder. This excluded the presence of water in air. Thus, the cooling of the substrate by hexane evaporation and possible condensation of water at ambient conditions did not play a significant role.

Figure 1b shows a typical pattern of water droplets formed in the central part of the film area spread on TEM grids covered with a NC film. The average diameter of the droplets $D_d \approx 0.5$ μm and their average height $h_d \approx 40-50$ nm were measured directly (in the range of 30 min) following formation of the droplet pattern (Figure 1c). A more detailed image of a water droplet is illustrated in Figure 2. After drying of the samples for 7 weeks, their height decreased to $h_d \approx 10$ nm, without a significant change of D_d (Figure 3). The remaining dropletlike deposit after complete drying of the droplets consisted of HDA. That was proven

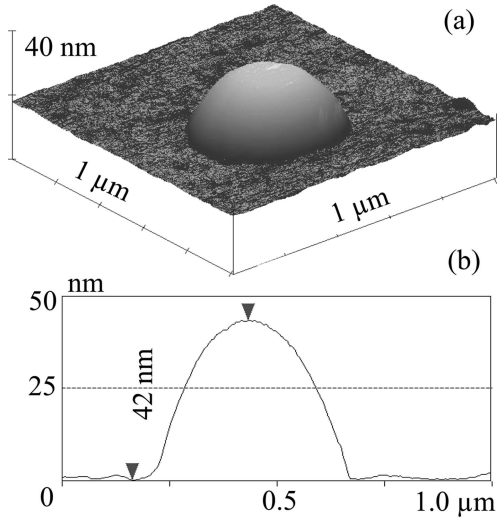

FIGURE 2. (a) Typical three-dimensional AFM height image of a water droplet taken directly after formation of the droplet pattern. This droplet is indicated by the box in Figure 1b. (b) Cross section of the droplet illustrated in part a.

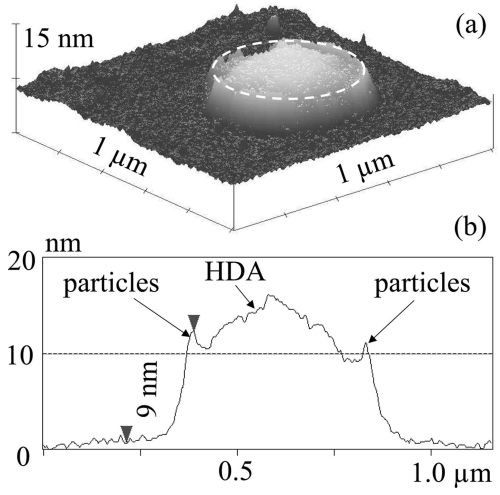

FIGURE 3. (a) Typical three-dimensional AFM height image of a HDA deposit remaining after drying of the water droplet for 7 weeks. The indicated dashed ring illustrates the location of a nanoparticle ring. (b) Cross section of the dropletlike HDA deposit surrounded by the $CoPt_3$ nanoparticle ring illustrated in part a. Initially, the nanoparticles were coated with a HDA monolayer (stabilizer), and their diameter amounts to 8.8 nm.

via a removal of the HDA deposit from the dry sample by immersing the sample for a period of 5 min in hexane, which is a selective solvent for HDA.

The analysis of the droplet patterns by TEM clearly demonstrated that the $CoPt_3$ particles self-assembled into ordered arrays located at the periphery of the droplets (Figures 4 and 5). It was found that the arrays with a different number of chains can be formed via variation of the particle concentration in the initial solution and via the size of the water droplets. For example, Figure 4 displays the rings composed of several arrays containing mainly one aligned chain of particles. Figure 5 displays the rings with mainly two (Figure 5a), three (Figure 5c), or four (Figure 5e) aligned chains of particles, respectively, with their lengths being about 100 nm. For example, from the analysis of the center-to-center distances and the particle radius, the distribution

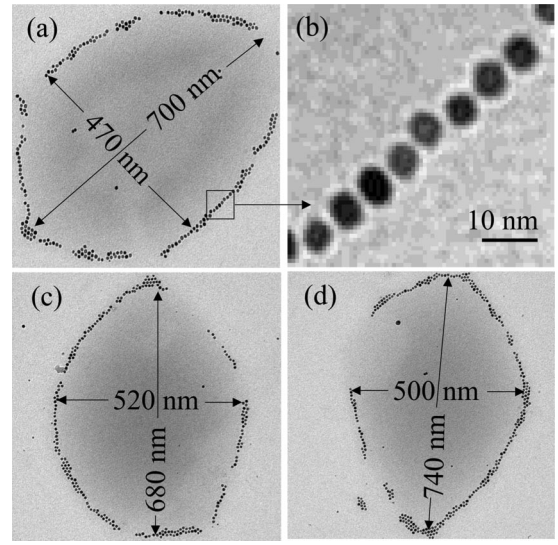

FIGURE 4. (a) TEM image of a $CoPt_3$ ring composed of several arrays containing mainly one chain. The ring was imaged before the removal of HDA from the sample. (b) Magnified image of the area indicated by the square box in part a. (c and d) TEM images of $CoPt_3$ rings after the removal of HDA from the sample. All three rings shown in parts a, c, and d locate on the same sample.

of interparticle spacing was obtained, resulting in 3.21 ± 0.45 nm for the array shown in Figure 5d. Note that Figure 5a illustrates the TEM image of the same droplet shown in Figure 3 (AFM analysis). The particle rings shown in Figure 4 were produced with a particle concentration of 2.4×10^{12} cm^{-3} in solution and the rings shown in Figure 5 with a concentration of 3.1×10^{12} cm^{-3}. For the constant concentrations of water and particles in the initial solution, the average size of particle rings (size of the water droplets) and length of the ordered chains of particles (about 100 nm) were always fairly reproducible in this experiment.

It should be noted that the ring shown in Figure 4a was imaged before and the rings shown in parts c and d of Figure 4 after the removal of HDA from the sample. It turned out that both the number and position of the individual nanoparticles did not change, which indicates that all particles in rings are situated at the interface between HDA and the NC layer after water evaporation and turned out to be somewhat embedded in the NC layer. In other words, the nanoparticles in the interior of the dry HDA deposit are only located on the interface with the NC layer but not in the rest of the HDA deposit volume. If the particles were not partially embedded in the NC layer, they would be washed off during the HDA removal (by immersing the sample in hexane).

4. SCENARIO OF THE NANOPARTICLE RING FORMATION

In accordance with the experimental results described above, it can be concluded that during hexane evaporation from the solution film (about 20 s) the subsequent processes occur: (a) the solution film transforms into a bilayer composed of a hexane layer on the water layer; (b) the hexane layer dewets the surface of the water layer; (c) during dewetting and evaporation of the hexane layer, most of nanoparticles and HDA existing in the hexane layer adsorb

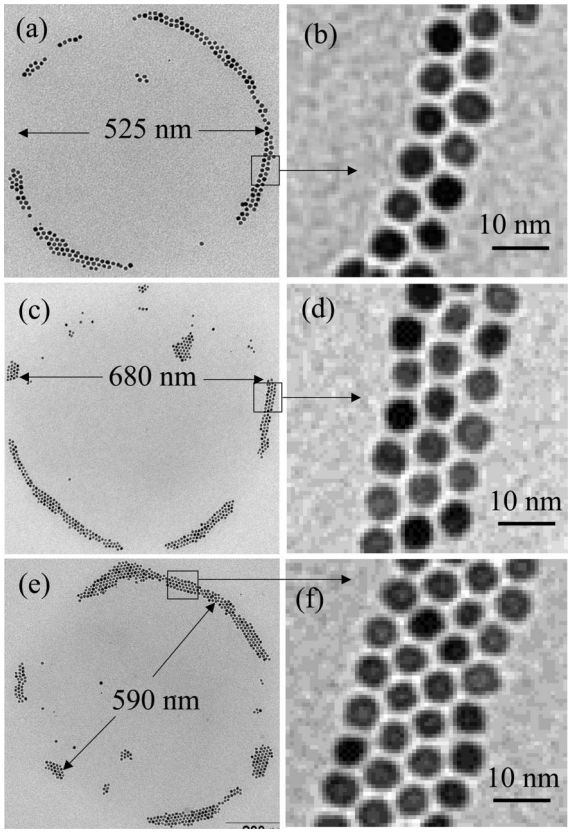

FIGURE 5. (a) TEM image of a $CoPt_3$ ring composed of several arrays containing mainly two chains. This image is taken from the same droplet as that shown in Figure 3a (AFM image). (b) Magnified image of the area indicated by the square box in part a. (c) TEM image of a $CoPt_3$ ring composed of several arrays containing mainly three chains. (d) Magnified image of the area indicated by the square box in part c. (e) TEM image of a $CoPt_3$ ring composed of several arrays containing mainly four chains. (f) Magnified image of the area indicated by the square box in part e. The rings in parts a and c locate on the same sample, but the ring in part e locates on the other one. All rings were imaged before the removal of HDA from the sample.

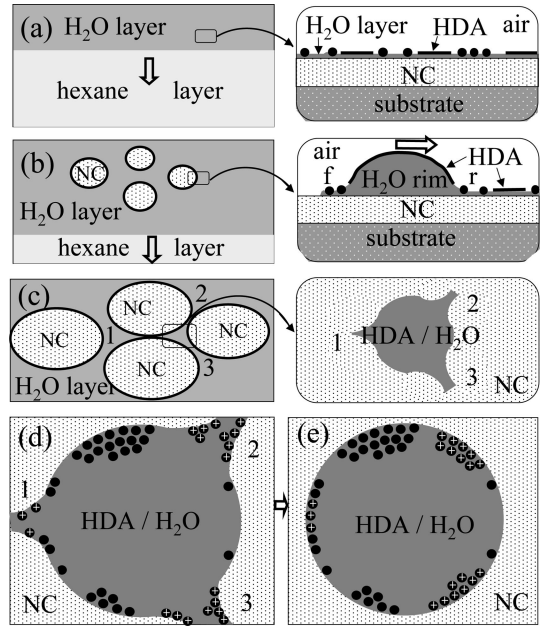

FIGURE 6. Schematic illustration of the development of close-packed particle arrays via the dewetting water layer. (a) Top view of the water layer formed on the NC-coated substrate after dewetting and evaporation of hexane. A magnified side view of the area indicated by the square box is shown on the right. The particles are denoted as circles and the HDA clusters as plates. (b) Development of the holes appearing in the dewetting water layer. A magnified side view of the rim forming in the dewetting water layer is shown on the right; f and r denote front and rear sides of the rim. (c) Formation of the cellular structure containing water ribbons. Formation of a water droplet from a fragment indicated by the square box is shown on the right. (d) Assembling of particles at the water droplet edge. The particles located at the ribbon edges are additionally denoted with white crosses. (e) Final formation of a water droplet with particles assembled at its edge.

on the surface of the water layer (nanoparticles and HDA are not soluble in water); (d) the water layer covered by nanoparticles and HDA dewets the surface of substrate (NC layer) and decomposes into droplets; (e) during dewetting, the particles locate at the rim edge of the dewetted water layer and follow its motion; (f) finally, during formation of the water droplets, the particles order along their edges. It should be noted that the events (a)−(f) indicated above must not be considered a sequence but a list of events that appear during hexane evaporation from the solution film consisting of hexane, water, HDA, and nanoparticles. Most of these events overlap or take place simultaneously.

Figure 6 schematically shows the mechanism responsible for the formation of the arrays of nanoparticles. Figure 6a shows the dewetting of the hexane layer on the surface of the water layer. The dewetting and evaporation of this layer (containing nanoparticles and HDA) during the time of 3 s can lead to strong hexane gradients between the bulk and contact line because hexane evaporates mostly near the air/hexane/water contact line. The difference between the surface tension of water (72.5 mN/m) and hexane (18.4 mN/m) creates a surface tension gradient between the bulk and contact line. The combination of two such gradients can induce a Marangoni flow of hexane from the bulk toward the contact line. The HDA and nanoparticles can follow the hexane flow (18−20) and adsorb along the contact line onto the surface of the water layer.

The water layer located on the NC layer is unstable and starts to dewet by forming holes (Figure 6b) because the spreading coefficient S_{01} is negative, $S_{01} = \gamma_1 - \gamma_0 - \gamma_{01} = -89$ mN/m (21). Here, $\gamma_1 = 38$ mN/m designates the surface tension of NC (at the boundary to air); $\gamma_{01} = 55$ mN/m is the interfacial tension between water and NC. The latter was calculated following Israelachvili (22) as $\gamma_{01} = \gamma_0 + \gamma_1 - 2(\gamma_{0d}\gamma_1)^{0.5}$ where $\gamma_{0d} = 20$ mN/m is the only dispersion force contribution to the surface tension of water. Note that the value of S_{01} estimated above for pure water on the NC film should only be considered a qualitative indicator. When the thin water layer is covered with HDA and nanoparticles, the reductions of γ_0 and γ_{01} have to be taken into account. During dewetting of the water layer, holes grow in the layer, and the removed water accumulates at the edge of the holes, building rims. The cross section of a rim is a portion of a circle (Figure 6b on the right). Because the front side f of the rim is moving, the particles located at this contact line have to follow its retraction and, consequently, assemble into the ordered arrays along the contact line. The holes become large enough so that their rims contact each other (Figure

6c). This results in the formation of ribbons, building the cellular structure. These ribbons are unstable and decompose into droplets. Most of the particles that were collected from the dewetted area assemble at the contact line of the water droplets (Figure 6d). Finally, the force governing the arrangement of particles into ordered assemblies is the capillary attraction because the thickness of the water layer at the droplet edge is comparable to the particle diameter (Figure 6e) (23).

In the following, a few details of the mechanism described above will be considered. The thickness of the initially formed water layer in the middle part of the spreading area can be determined from Figure 1b, where 81 droplets on the $10 \times 10\ \mu m^2$ area are located. That means that on an average water of the area of $1.23\ \mu m^2$ was accumulated for the formation of one water droplet. The volume of one droplet can be estimated by $V_d = \pi D_d^2 h_d/8$. The equation yields $V_d \approx 4.4 \times 10^{-21}\ m^3$ for the experimentally obtained average values $D_d \approx 0.5\ \mu m$ and $h_d \approx 45$ nm (Figure 1c). The corresponding volume of the dropletlike HDA deposit formed after evaporation of water from the droplet amounts to about $1.0 \times 10^{-21}\ m^3$ for the experimentally obtained diameter of the HDA deposit $D_{HDA} \approx 0.5\ \mu m$ and their height $h_{HDA} \approx 10$ nm (Figure 3). For example, the volume of all 192 nanoparticles illustrated in Figure 5a amounts to about $6.8 \times 10^{-23}\ m^3$ for the $CoPt_3$ particles coated with the HDA monolayer (stabilizer) whose diameter amounts to 8.8 nm. Excluding the volume of the HDA deposit and nanoparticles, the resulting thickness of the water layer initially spreading onto the area of $1.23\ \mu m^2$ and then accumulating into a droplet with the volume $3.3 \times 10^{-21}\ m^3$ amounts to about 3 nm. Deduced from the concentration of water in solution (0.015 vol %), an 11-nm-thick water layer was expected on average. First, this difference can be explained to be due to the water evaporation that took place during the time span between spreading of the initial solution and the AFM measurements. Second, the thickness of the water layer at the edge of the spreading area is larger than that in the central part. It is obvious because the experimentally observed diameter of the polygons building the cellular water structure before it decomposes into droplets is larger at the edge of the spreading area (Figure 1a) compared to that in the central part. Third, it is possible that the additional water (0.01 vol %) is not completely dissolved in hexane (which itself contains 0.005 vol % of water).

The experimentally determined volume $1.0 \times 10^{-21}\ m^3$ of the HDA deposit adsorbed on the water layer area of 1.23 μm^2 after hexane evaporation can cover the water layer with a continuous film of about 0.8 nm thickness. Deduced from the concentration of HDA in solution (0.001 vol %), a layer of about 0.8 nm thickness was expected on average, which is in good agreement with the experimentally estimated value. The HDA molecules can adsorb on the water surface either as a monolayer with a discrete thickness of 1.4 nm (length of the HDA molecule) or as micelles with a thickness of 2.8 nm (two monolayers), which order into the larger clusters then (24). That means that only $0.71\ \mu m^2$ of the water layer area of $1.23\ \mu m^2$ can be covered with a 1.4-nm-thick HDA layer. If HDA forms micelles on the water layer, the covered area will still be smaller. The corresponding area of the water layer covered, for example, with 192 nanoparticles (Figure 5a) amounts to $0.01\ \mu m^2$. That means that only 58 % of the water layer area of $1.23\ \mu m^2$ can be covered with HDA and particles. This situation changes significantly, when the water layer with an area of $1.23\ \mu m^2$ and a thickness of 3 nm deforms to the water droplet. The surface area of the water droplet can be estimated by $A_d = \pi D_d[(D_d^2/4 + 4h_w^2)^{3/2} - D_d^3/8]/12h_w^2$. The equation yields $A_d \approx 0.2\ \mu m^2$ for the experimentally obtained average values $D_d \approx 0.5\ \mu m$ and $h_w \approx 35$ nm. After formation of the water droplet, HDA is located on the surface. In other words, HDA cannot be distributed in the interior of the water droplet because HDA is not soluble in water. As a result, the available amount of HDA would cover the surface of the water droplet with a smooth film of about 5 nm thickness. During evaporation of water from the droplet, its surface area decreases and, finally, HDA deforms to the dropletlike deposit whose thickness amounts to about 10 nm (after complete evaporation of water).

An important question to address is the following: What if most of the HDA forms a molecularly thin film on the NC film after dewetting and evaporation of the hexane layer? In this case, the HDA molecules located on the NC layer could be moved from the place where they adsorbed to the place where the water droplets formed only with the contact line of the dewetting water layer. If that occurs, most of the HDA molecules can be expected to found together with the nanoparticles at the periphery of the droplet; i.e., the cross section of the HDA deposit left after water evaporation should have a cuplike shape. However, that is not in accordance with the experimental observation shown in Figure 3b, where a dropletlike profile of the HDA deposit is observed. Accordingly, the HDA molecules did not follow the motion of the contact line of the dewetting water layer; i.e., after dewetting and evaporation of the hexane layer, most of the HDA existing in solution adsorbs on the surface of the water layer.

An interesting conclusion may be drawn considering Figures 4 and 5: Only a few particles can be seen within the ringlike structures. Similar images were observed for more than 100 specimens. Experimentally, originating from the concentration of particles in the solution, about two or three nanoparticles on an area of $100 \times 100\ nm^2$ of the spread film were expected. However, this is obviously not in accordance with the experimental results shown in Figures 4 and 5, where selected regions contain significantly more particles and almost no particles are found within the ringlike structures. That means that during dewetting most nanoparticles order at the rim edge of the dewetted water layer; i.e., the nanoparticles cannot be distributed in the interior of the water rim because they are not soluble in water. As a result, during dewetting and droplet formation, the nano-

particles are located at the droplet edge, where they contact the NC layer and, finally, pin it.

5. CONCLUSION

It has been experimentally demonstrated that, during the hexane evaporation from a thin film of a hexane solution containing $CoPt_3$ particles, HDA, and water, the following processes occur: Water separates from hexane and, after hexane evaporation, forms a thin layer on the substrate. Dewetting of this thin water layer from the substrate leads to the formation of droplets. Particles located at the contact line of the dewetting water layer follow its motion and thus assemble into ordered arrays at the periphery of the water droplets.

Acknowledgment. The author thank G. Reiter, G. H. Bauer, and J. Parisi for valuable discussions of the experimental results and E. Shevchenko for preparing $CoPt_3$ particles. This work was financially supported by the Deutsche Forschungsgemeinschaft under Grant PA 378/10-1.

REFERENCES AND NOTES

(1) Delft, J.; Ralf, D. C. *Phys. Rep.* **2001**, *345*, 61.
(2) Parthasarathy, R.; Lin, X. M.; Jaeger, H. M. *Phys. Rev. Lett.* **2001**, *87*, 186807.
(3) Morgan, N. Y.; Leatherdale, C. A.; Drndic, M.; Jarosz, M. V.; Kastner, M. A.; Bawendi, M. *Phys. Rev. B* **2002**, *66*, 075339.
(4) Yu, D.; Wang, C. J.; Wehrenberg, B. L.; Guyot-Sionnest, P. *Phys. Rev. Lett.* **2004**, *92*, 216802.
(5) Elteto, K.; Lin, X. M.; Jaeger, H. M. *Phys. Rev. B* **2005**, *71*, 205412.
(6) Kaplan, D. M.; Sverdlov, V. A.; Likharev, K. K. *Phys. Rev. B* **2003**, *68*, 045321.
(7) Fogler, M. M.; Teber, S.; Shklovskii, B. I. *Phys. Rev. B* **2004**, *69*, 035413.
(8) Semrau, S.; Schoeller, H.; Wenzel, W. *Phys. Rev. B* **2005**, *72*, 205443.
(9) Wyrwa, D.; Beyer, N.; Schmid, G. *Nano Lett.* **2002**, *2*, 419.
(10) Huang, J.; Tao, A. R.; Connor, S.; He, R.; Yang, P. *Nano Lett.* **2006**, *6*, 524.
(11) Suematsu, N. J.; Ogawa, Y.; Yamamoto, Y.; Yamaguchi, T. *J. Colloid Interface Sci.* **2007**, *310*, 648.
(12) Khanal, B. P.; Zubarev, E. R. *Angew. Chem.* **2007**, *119*, 2245.
(13) Govor, L. V.; Reiter, G.; Parisi, J.; Bauer, G. H. *Phys. Rev. E* **2004**, *69*, 061609.
(14) Govor, L. V.; Parisi, J.; Bauer, G. H.; Reiter, G. *Phys. Rev. E* **2005**, *71*, 051603.
(15) Govor, L. V.; Reiter, G.; Bauer, G. H.; Parisi, J. *Phys. Rev. E* **2006**, *74*, 061603.
(16) Shevchenko, E.; Talapin, D.; Kornowski, A.; Rogach, A.; Weller, H. *J. Am. Chem. Soc.* **2002**, *124*, 11480.
(17) Demond, A. H.; Lindner, A. S. *Environ. Sci. Technol.* **1993**, *27*, 2318.
(18) Vuilleumier, R.; Ego, V.; Neltner, L.; Cazabat, A. M. *Langmuir* **1995**, *11*, 4117.
(19) Fanton, X.; Cazabat, A. M. *Langmuir* **1998**, *14*, 2554.
(20) Cai, Y.; Newby, B. Z. *J. Am. Chem. Soc.* **2008**, *130*, 6076.
(21) Adamson, A. W. *Physical Chemistry of Surfaces*; Wiley: New York, 1982.
(22) Israelachvili, J. N. *Intermolecular and Surface Forces*; Academic Press: London, 1991.
(23) Kralchevsky, P. A.; Denkov, N. D.; Paunov, V. N.; Velev, O. D.; Ivanov, I. B.; Yoshimora, H.; Nagayama, K. *J. Phys.: Condens. Matter* **1994**, *6*, A395.
(24) Govor, L. V.; Reiter, G.; Bauer, G. H.; Parisi, J. *Phys. Lett. A* **2006**, *353*, 198.

AM800151E